Incorporation of Rayleigh lines into Joule cycle processes to allow for heating pressure drops

E.A. Bunt [1]

(First received December 1994; Final version March 1995)

Abstract

Rayleigh lines, representing states of constant mass flux per unit area when heat is transferred to or from a gas, are proposed for use in a modified open or closed Joule cycle (to replace lines of constant pressure) to better describe cases such as regenerative heat transfer and reheating, as well as combustion processes in jet engines, by allowing for pressure drops during heating. The application of Rayleigh lines for this purpose is simplified by the fact that at low subsonic Mach numbers, lines for different mass velocities (which may result from varying mass flow or combustion chamber area) tend to coincide. The efficiency of such a modified Joule cycle is derived.

Nomenclature

a	$\eta_t \eta_c \theta$
A	cross-sectional area of duct
b	$\eta_c (\theta - 1)$
e	regenerator effectiveness
G	mass velocity
K	$1 + (\gamma - 1) M^2/2$
K_1, K_2	constants in pressure loss factor (PLF)
$\dot{m}$	mass flow
M	Mach number
p	pressure
PLF	pressure loss factor
Q	heat flux
R	gas content
s	entropy
T	temperature
v	specific volume $(= 1/\rho)$
V	velocity
W	work

Greek

α	pressure ratio p_2/p_1
γ	ratio of specific heats
η	efficiency
θ	temperature ratio T_3/T_1
ρ	mass density
τ	temperature ratio T_2/T_1

Subscripts

a	atmospheric
c	compressor
t	stagnation; turbine
*	thermal choking condition
1	upstream
2	downstream

Superscript

$(')$	state after non-isentropic change

Introduction

The simple Joule or Brayton cycle, consisting of two constant pressure lines and two isentropes (all usually expressed in terms of static parameters) has long been taken as the theoretical basis of operation of ramjet and gas turbine engines – as illustrated, for example, by a-b-c-d in the p-v diagram of Figure 6. In practice, the experimental cycle may be somewhat different. Not only are the expansion and compression processes non-isentropic, but the actual combustion process involves a pressure drop, as shown, for example, by the experimental values of Figure 6. Whilst the overall effect of such a compression process, although complex, is not too different from that of an isentropic process, the fact that the pressure drop during heating (not normally considered in the simple theoretical cycle) is approximately linear on a p-v diagram suggests that it may be considered in terms of Rayleigh heating flow which also predicts such a pressure drop. This paper examines the possibility of incorporating a Rayleigh heating or cooling line into processes normally described by the standard Joule cycle, as given in standard texts, e.g. [1;2;3;4;5;6;7], and takes into account the practical aspect of variation of mass flow or heating chamber area in relation to the use of such curves. The difference between Rayleigh curves on T-s and T_t-s ordinates (which is often overlooked) is also emphasised.

Some properties of T-s, h-s, and p-v plots

Rayleigh lines

For a constant area duct, with continuity, in one-dimensional flow, without friction, and using perfect gas analysis, $G = \rho V =$ constant. Applying the momentum equation, $A\left(p + \rho V^2\right) =$ constant, we have $p + G^2/\rho =$

[1]School of Mechanical Engineering, University of the Witwatersrand, P.O. Wits, 2050 Republic of South Africa

constant, the equation of a Rayleigh line. This may be written $p_1 - p_2 = (v_2 - v_1)\,G^2$ or $\frac{(p_1-p_2)}{(v_1-v_2)} = -G^2$, which is linear on a p-v plot. Also, taking $T = \frac{pv}{R}$ and $V = \frac{G}{\rho} = Gv$,

$$\Rightarrow M = Gv / \sqrt{\gamma RT} = G\sqrt{v / \gamma p} \quad \text{while} \qquad (1)$$

$$T_t = T\left(1 + \frac{\gamma - 1}{2} M^2\right) = T + v^2 (\gamma - 1)\, G^2 / 2\gamma R\,. \qquad (2)$$

For a heat addition process 2-3, as shown in, for example, Figure 4,

$$\begin{aligned} s_3 - s_2 &= \frac{R\gamma}{\gamma - 1} \ln\left[\frac{T_3}{T_2}\left(\frac{p_2}{p_3}\right)^{\frac{\gamma-1}{\gamma}}\right] \qquad (3) \\ &= \frac{R\gamma}{\gamma - 1} \ln\left[\frac{v_3}{v_2}\left(\frac{p_3}{p_2}\right)^{\frac{1}{\gamma}}\right] \end{aligned}$$

and in terms of M, we have

$$s_3 - s_2 = \frac{R\gamma}{\gamma - 1} \ln\left[\frac{M_3^2}{M_2^2}\left(\frac{1 + \gamma M_2^2}{1 + \gamma M_3^2}\right)^{\frac{\gamma+1}{\gamma}}\right] \quad \text{and} \qquad (4)$$

$$T_3 = T_2 \frac{M_3^2}{M_2^2}\left(\frac{1 + \gamma M_2^2}{1 + \gamma M_3^2}\right)^2 \qquad (5)$$

In terms of the thermal choking (*) conditions ($M = 1$), we also have, for $K \equiv 1 + (\gamma - 1)\ M^2/2$, so that $K* \equiv (\gamma + 1)/2$:

$$p_t / p_t^* = \left(\frac{p}{p^*}\right)\left(\frac{K}{K^*}\right)^{\frac{\gamma}{\gamma-1}} = \frac{\gamma + 1}{1 + \gamma M^2}\left(\frac{K}{K^*}\right)^{\frac{\gamma}{\gamma-1}} \qquad (6)$$

$$T_t / T_t^* = \left(\frac{T}{T^*}\right)\left(\frac{K}{K^*}\right) = \left(\frac{M(\gamma + 1)^2}{1 + \gamma M^2}\right)^2 \left(\frac{K}{K^*}\right) \quad \text{and} \qquad (7)$$

$$\rho_t \rho_t^* = \left(\frac{\rho}{\rho^*}\right)\left(\frac{K}{K^*}\right)^{\frac{1}{\gamma-1}} = \left(\frac{1 + \gamma M^2}{(1 + \gamma)\, M^2}\right)\left(\frac{K}{K^*}\right)^{\frac{1}{\gamma-1}} \qquad (8)$$

The Mach number at entry to the combustion chamber of a turbojet engine may vary from 0.07 to 0.22,[2] but calculations based on examples in [4] point to a value of 0.2 as being typical. As a result, the value of M may increase during combustion to approximately 0.5 (less after afterburning). Although at low Mach numbers the difference between T and T_t is often ignored, T_t / T for $M = 0.5$ is 1.05. Since the addition of heat to a moving gas in a combustion chamber is easily represented as an increase in enthalpy, a T-s diagram may often be more suitable to depict Rayleigh lines on an actual cycle. T_t-s curves corresponding to T-s curves may be found by putting

$$T_t = \left(1 + \frac{\gamma - 1}{2} M^2\right) T \qquad (9)$$

whence for example,

$$T_{t_3} = \left(1 + \frac{\gamma - 1}{2} M_3^2\right) T_2 \frac{M_3^2}{M_2^2}\left(\frac{1 + \gamma M_2^2}{1 + \gamma M_3^2}\right)^2 \qquad (10)$$

Figure 1 compares Rayleigh lines in T-s and T_t-s forms as indicated by $R(T)$ and $R\,(T_t)$, s being already a 'stagnation' concept. The overall T_t-s diagram differs from the T-s diagram in that the supersonic branch of the Rayleigh line lies above the subsonic branch, and better emphasises the large enthalpy input needed to decelerate a gas moving with supersonic velocity than is apparent on a T-s plot.

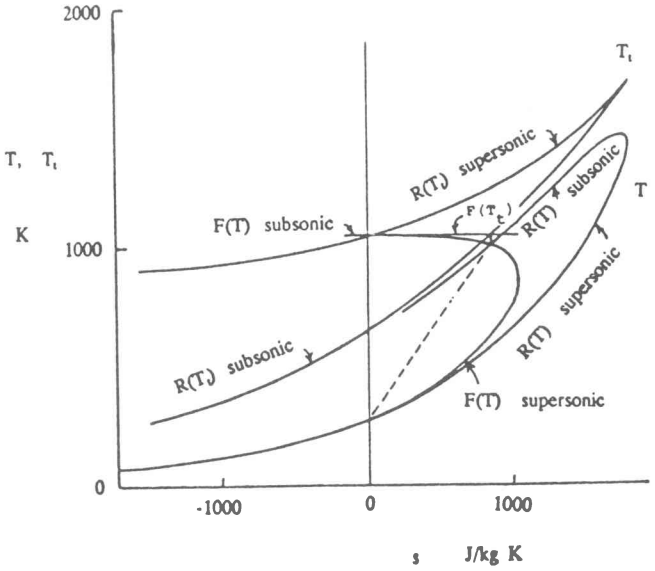

Figure 1 Comparison of T-s and T_t-s lines
$F(T)$, $F(T_t)$ Fanno lines, $R(T)$, $R(T_t)$ Rayleigh lines
---- Normal shock

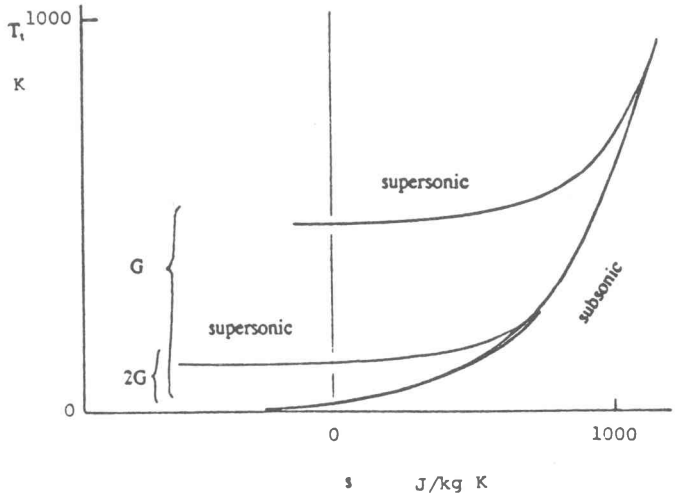

Figure 2 Rayleigh lines on T_t-s diagram for two values of G

Fanno lines

Rayleigh lines are often considered together with the lines representing Fanno flow, representing adiabatic flow in a constant area duct with friction. Fanno lines are thus lines of constant stagnation temperature, and hence of constant stagnation enthalpy: $h_t = h + V^2/2 = h + \gamma RTM^2/2$.

Writing $C_pT_t = C_pT + V^2/2$, then since $G = V/v$, $C_p = \gamma R/(\gamma - 1)$, and $pv = RT$,

$$C_pT_t = \frac{\gamma}{\gamma - 1}pv + G^2v^2/2 = \text{constant} \qquad (11)$$

whence, in terms of M, between, say points 2 and 3, with T_t constant,

$$s_3 - s_2 = R \ln \left\{ \frac{M_3}{M_2} \left(\frac{K_2}{K_3} \right)^{\frac{\gamma+1}{2(\gamma-1)}} \right\} \qquad (12)$$

The intersections of Rayleigh and Fanno lines represent the end points of a normal shock, such as occurs in (or upstream of) a supersonic intake – as illustrated in Figure 1. On the T_t-s plot, a Fanno line will be horizontal. The normal shock transition from the supersonic to the subsonic branches of a Fanno curve is now represented by a section of this horizontal line.

Effect on Rayleigh Lines of $\dot{m}$ and A changes

A simplified approach to this topic is as follows. The above normally considers that $\dot{m}$ and A are constant in a heat transfer duct; however, 'secondary' and 'tertiary' air may enter, or be bled from, a duct during operation, while A may change for design reasons. It is therefore of interest to consider the practical behaviour of Rayleigh curves when such changes occur. For constant A, a different value of $\dot{m}$ will give a proportionately different value of G, resulting in a different Rayleigh line; Figure 2 shows Rayleigh lines plotted on T_t-s ordinates for appropriate values of $\dot{m}$ and $2\dot{m}$. The low subsonic branches of curves of widely differing G values are seen to be closely coincident (as a result of the kinetic contribution to T_t) and Rayleigh lines are thus a useful way of representing the heating process in the combustion chamber on a temperature-entropy diagram when $\dot{m}$ varies under these conditions. As will be seen later (Figure 3), the subsonic branches of different G curves on T-s ordinates also tend to coincide at low subsonic Mach numbers. This convergence is useful when using Rayleigh lines under conditions, for example, of combustion chamber geometry variation. This close correspondence of the subsonic curves for different values of G during heat addition does not, of course, apply in the supersonic heat addition case – except at unrealistically high Mach numbers as the curves approach the s-axis asymptotically. However, the Mach numbers corresponding to closely adjacent points for different G curves are not, of course, the same; for example, if G is doubled, M will be approximately doubled for the same stagnation temperature condition at starting, since from the mass velocity equation, using

$$K = 1 + \frac{\gamma - 1}{2}M^2 \qquad (13)$$

$$\begin{aligned} \Rightarrow G &= \rho V = \rho_t \left(\tfrac{1}{K}\right)^{\frac{1}{\gamma-1}} M\sqrt{\frac{\gamma RT_t}{K}} \\ &= M\rho_t\sqrt{\gamma RT_t}\left(\tfrac{1}{K}\right)^{\frac{(\gamma+1)}{2(\gamma-1)}} \end{aligned} \qquad (14)$$

For $\gamma = 1.4$, this leads to $M/(5 + M^2)^3 = \text{constant} \times G$, the constant relating to the given stagnation condition. (The denominator of this term is obviously only a weak function of M if the latter is subsonic.) [2]

If the area changes at constant $\dot{m}$, consider the equation of continuity in the form

$$\dot{m} = AV\rho = GA = \text{constant} \qquad (15)$$

If, for example, A is halved, G is doubled, and a shift to a curve as for a correspondingly increased value of $\dot{m}$ occurs. These effects are consistent with the use of an increased size of nozzle in a gas turbine engine with reheat to permit the use of higher nozzle entrance temperatures.[4]

Worked example

Figure 3(a) shows a typical Rayleigh line (dashed) on T-s ordinates, starting at $M = 0.2$, and for which $G = 181.56$ kg/m^{2}s. The two additional curves shown for 1.5 G and 2 G correspond to starting Mach numbers of 0.2973 and 0.4166 for the same stagnation temperature of $T_{t_2} = 394$ K. The corresponding effect of a G change on the p-v diagram is illustrated in Figure 3(b); in the case shown, the upper curve starts at a very low value of M. A change in G brings about a change of slope as the combustion chamber mass flow or area changes. For any given mass flow, the pressure drop is obviously greater for a duct of smaller area (or for an increase of mass flow in a duct of constant area).

Pressure effects

The entropy change on a line of constant pressure between points 2 and 3 is given by putting $p_2 = p_3$ in

$$\Delta s = \frac{R\gamma}{\gamma - 1} \ln \left\{ \frac{T_3}{T_2} \left(\frac{p_2}{p_3} \right)^{\frac{\gamma-1}{\gamma}} \right\} \qquad (16)$$

An example of such a line (for $p = 2.58$ bar) is given in Figure 3(a) for comparison with a Rayleigh line starting at the same point. On the other hand, the pressure drop during heating, $\Delta p_t/p_t$, is expressed [4] as

$$\begin{aligned} \frac{\Delta p_t}{p_t} &= \frac{(PLF)}{2A^2} \times \frac{\dot{m}(RT_t)}{p_t^2} \\ \text{where} & \\ PLF &= \frac{\Delta p_t}{\dot{m}^2/2\rho A^2} = K_1 + K_2\left(\frac{T_{t_3}}{T_{t_2}} - 1\right) \end{aligned} \qquad (17)$$

The pressure loss expression (PLF) involves a constant 'cold loss' factor K_1 (due to friction) and a 'fundamental pressure loss' involving K_2, due to the increase of temperature as a result of combustion (and hence, a function of T_{t_3}/T_{t_2}). This form of expression for $\Delta p_t/p_t$ introduces the variable $\dot{m}/A\,(= G)$, and in practice the value of $\dot{m}/A$ is chosen to yield a value of $\Delta p_t/p_t$ between 4 and 7%.[4]

[2] This expression was given by Çambel in [8] and [9].

Rayleigh lines (or a corresponding value of G) may thus be selected to conform to an appropriate value of $\Delta p_t / p_t$.

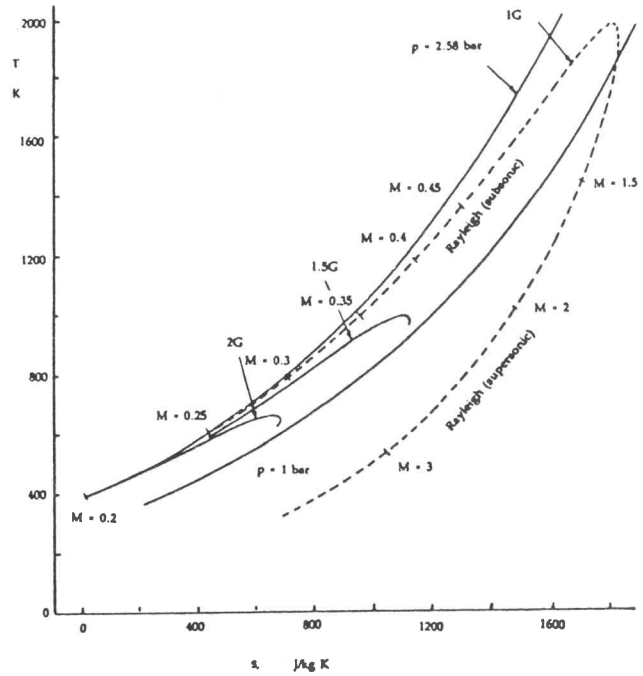

Figure 3(a) T-s plot for different G values
$G = 181.56$ kg/m^{2}s, $1.5\,G = 271.34$ kg/m^{2}s
$2\,G = 363.12$ kg/m^{2}s

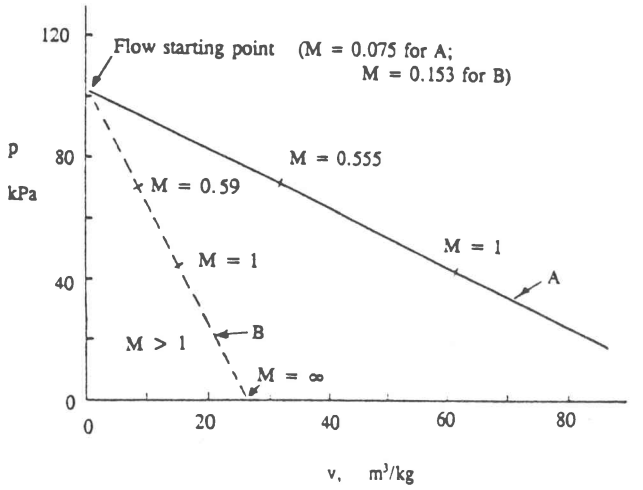

Figure 3(b) p-v plot for different G values
Curve A: $G = 31.42$ kg/m^{2}s, Curve B: $G = 62.84$ kg/m^{2}s

Applications of Rayleigh lines

Regenerative heat transfer

Consider a heat exchanger of the form shown in Figure 4(a). In the regenerator, Sections 2-3 and 5-6 will in general represent different geometries and hence different values of G. In general, T_3-$T_2 = e\,(T_5$-$T_6)$ if the specific heats are cancelled, and e is the regenerator effectiveness. In the ideal case ($e = 1$), $T_3 = T_5$ and $T_2 = T_6$. The ideal situation is depicted in Figure 4(a). The Rayleigh curve, R_1, corresponding to the heating section of the heat exchanger is here almost identical with that (R_2) for the combustion chamber. After point 5, cooling takes place in the other section of the heat exchanger – which corresponds to a different Rayleigh curve, R_3. For simplicity, M_5 has been made equal to M_3. At exit from the heat exchanger at 6, the flow will theoretically be at a higher pressure than p_5 and a drop to $p_7 (= p_a)$ is then required (shown as an isentropic drop).

In the calculation of the p-v diagram (Figure 4(b)), point 5 is found from the intersection of the isentropic line from 4 with the isothermal from 3; the Rayleigh line, R_3, (having the same value of G as for line 2-3) then extends to meet the isothermal from 2 at 6, from where 6-7 is the final isentropic drop.

Worked example

In Figure 4, the plot is based on a starting value of $T_1 = 280.1$ K, with $\tau = 2$. T_2 is taken as 560.2 K ($= T_6$) and $M_2 = 0.1$, while T_5 (after the drop through the turbine = 951 K ($= T_3$). $M_5 = M_3 = 0.132$. $M_6 = 0.1$.

Reheating

The process followed is that shown in Figure 5(a) and (b). The change of Rayleigh curves is here different from that shown for area change in Figure 3 since the presence of the turbine gives rise to a temperature discontinuity in the cycle; reheating therefore corresponds to a Rayleigh line starting at a different temperature point, and the resulting curve does not coincide with that relating to the chamber upstream of the turbine.

Worked example

In the case shown. we assume $M_2 = 0.2$. Then for

$p_{t_2} = 6.67$ bar
$T_{t_2} = 564.5$ K
$T_{t_3} = 1\,200$ K and
$T_2 = 560.0$ K

we have $\rho_3 = 1.77$ kg/m^3
$V_3 = 118.1$ m/s and
$M_3 = 0.312$

Then, $G = 383.3$ kg/m^{2}s. If the temperature through the turbine falls to $T_{t_4} = 959$ K and the area ratio A_3/A_4 is assumed to be 0.5, this gives $G_4 = (A_3/A_4)V_3\rho_3 = 104.5$ kg/m^{2}s, which defines the second Rayleigh curve. Let $T_{t_6} = 2\,000$ K after reheating. Then,

$$\begin{aligned} G &= 104.5 \text{ kg/m}^2\text{s} &&= V_4\rho_4 \\ &= M_4\,(\gamma RT_4)^{\frac{1}{2}}\,\rho_4 &&= M_4\,(\gamma\,/\,R)^{\frac{1}{2}}\,p_4\,/\,(T_4)^{\frac{1}{2}} \\ &= M_4\,(\gamma\,/\,R)^{\frac{1}{2}}\,\rho_{t_4} &/\;&(T_{t_4})^{\frac{1}{2}}\,K_4^{\frac{-(\gamma+1)}{2(\gamma-1)}} \end{aligned} \tag{18}$$

Since $T_4 = T_{t_4}/K_4$ and $p_4 = p_{t_4}/K_4^{\frac{\gamma}{\gamma-1}}$.

$\Rightarrow M_4 = 0.204$, leading to $M_6 = 0.31$.

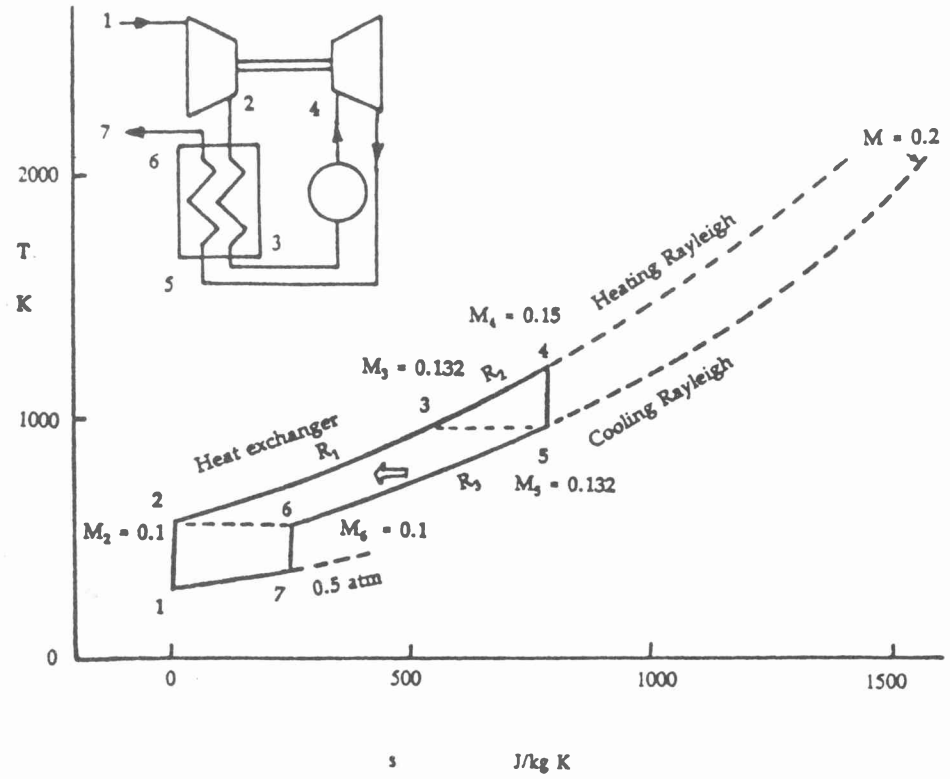

Figure 4(a) T-s diagram for a case of regenerative heat transfer.

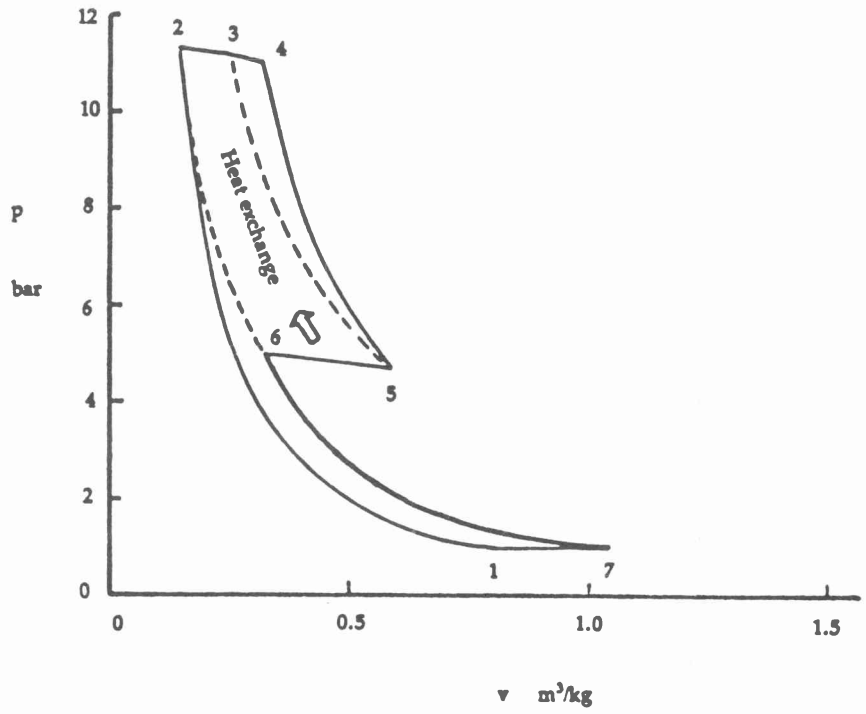

Figure 4(b) p-v diagram for a case of regenerative heat transfer.

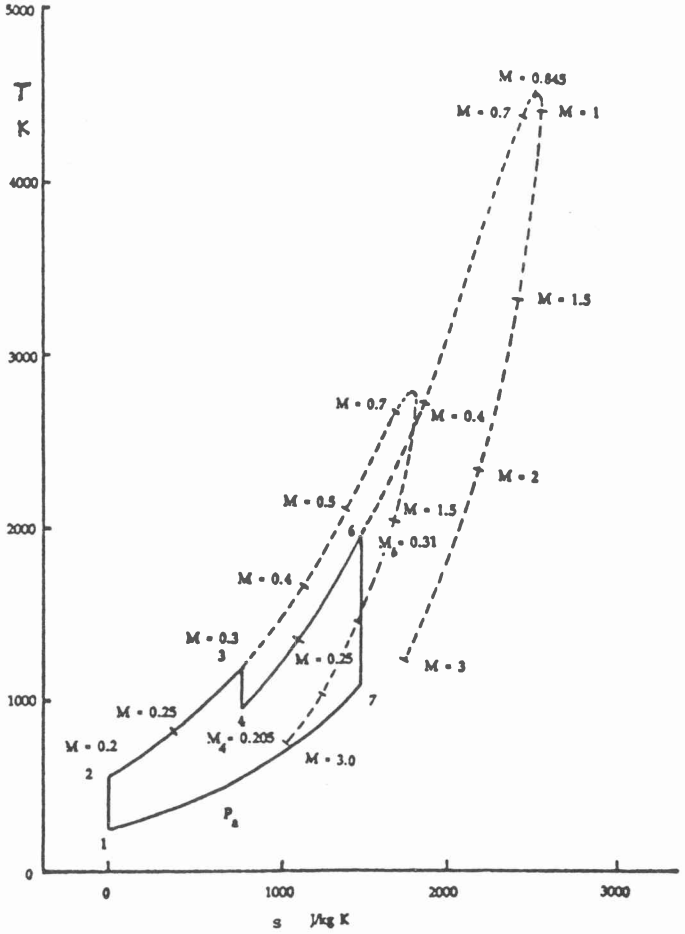

Figure 5(a) T-s diagram for a case of reheating (in a gas turbine).

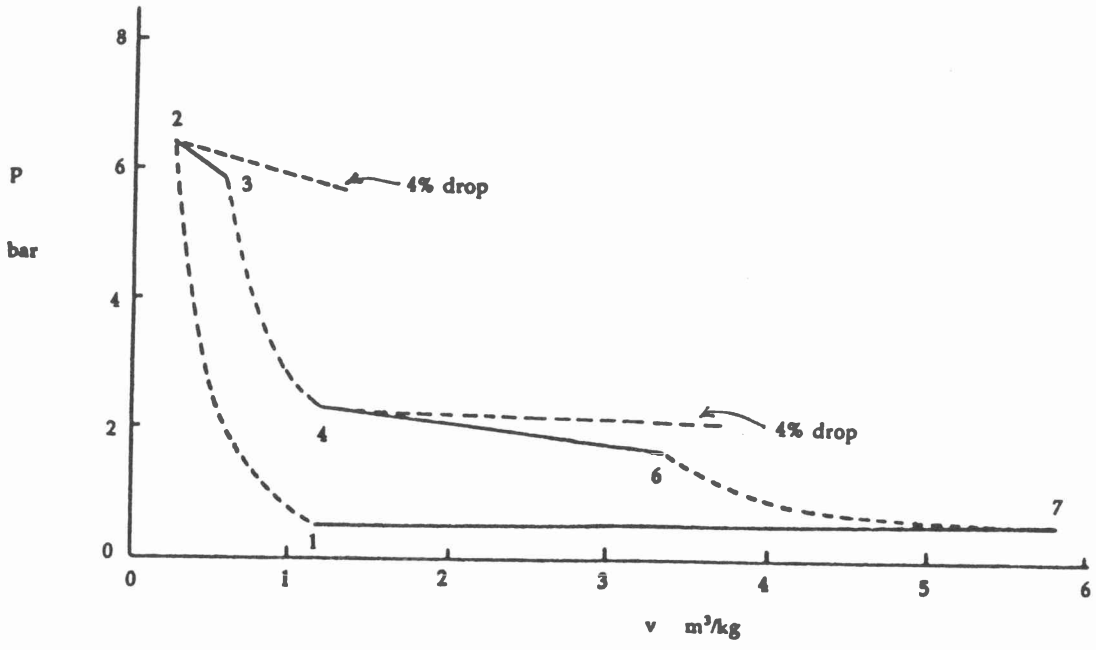

Figure 5(b) p-v diagram for a case of reheating (in a gas turbine).

The cycle is completed as shown in Figure 5(a) and a complete Rayleigh curve corresponding to the reheating process is given (of higher T_t^*). Figure 5(b) shows the corresponding pressure drops (7.8% from 2→3 compared with 27.7% from 4→6).

Supersonic intake phenomena

In general, compression is accomplished by one or more of the sequential processes indicated on Figure 6:

- Oblique shock compression;
- Supersonic diffusion;
- Normal shock compression; and
- Subsonic diffusion.

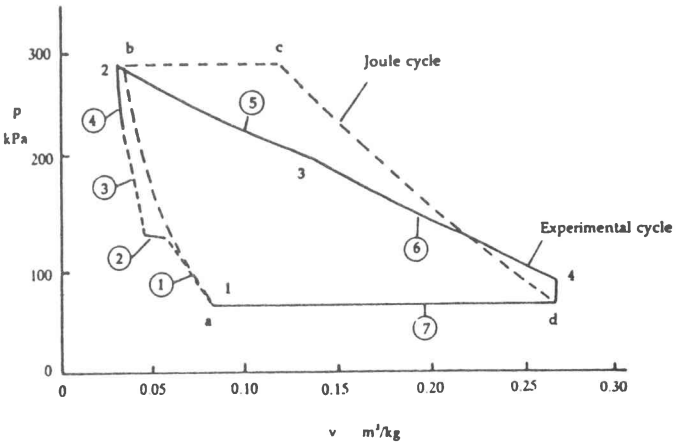

Figure 6 Theoretical and experimental Joule cycles (from [1])
Processes: 1. Oblique shock compression; 2. Supersonic diffusion; 3. Normal shock compression; 4. Subsonic diffusion; 5. Combustion; 6. Expansion; 7. Cooling. The experimental points are plotted from data given in [2] (corrected).

In a turbojet, these processes may be followed by further compression in the compressor unit. Although the overall process involving the above is not strictly a simply Rayleigh process (i.e. one associated merely with a stagnation temperature change), Figure 1, showing a transition in a duct from supersonic flow to subsonic flow through a normal shock, followed by subsonic heating, lends itself to illustrating several of the intake phenomena involved within the flow boundaries. The appropriate diagram is shown in Figure 7(a), and includes two Rayleigh lines, R_1 and R_2,which correspond to the different 'duct' areas. The oblique shock may be represented as reaching the outer rim of the intake duct (to avoid flow spillover – the shock-on-rim case). The flow area decreases in the supersonic region; the friction effects here result in changes closely similar to those occurring along a Fanno line. The normal shock shown (and the defining Fanno line) results from a flow Mach number not much greater than unity; downstream of the normal shock, the cross-sectional area normally enlarges to decelerate the now subsonic gas stream (equivalent to a decreasing value of G). The characteristic convergence of the two subsonic parts of the Rayleigh lines representing the different values of G will be noted.

The entropy zero is here taken at the station upstream of the normal shock, rather than at point 2 in the open cycle.

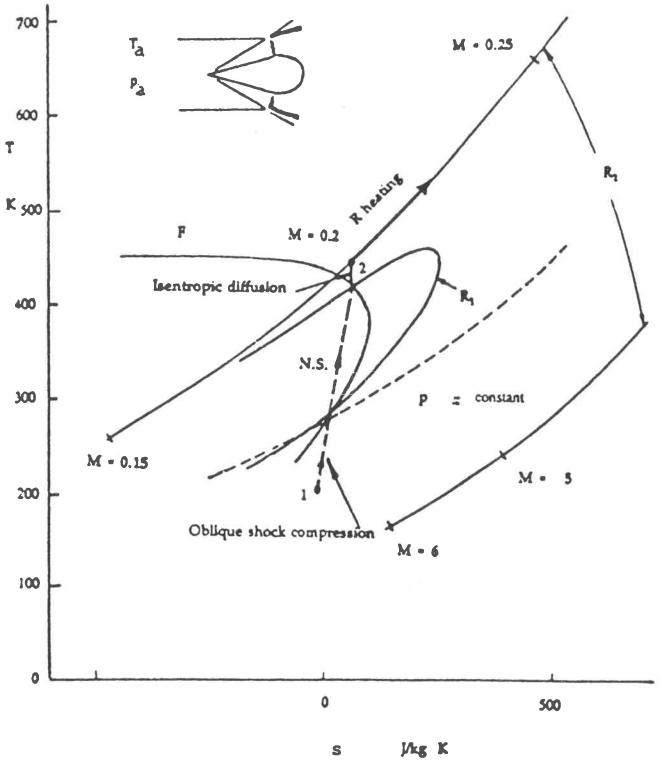

Figure 7(a) T-s diagram illustrating intake processes

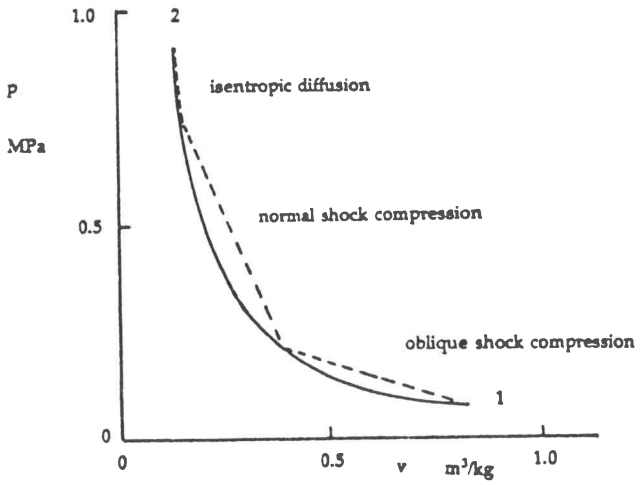

Figure 7(b) p-v diagram illustrating intake processes

Worked example

A simple 2-dimensional intake is chosen for purposes of illustration. The compression process starts at an assumed

freestream Mach number of 2.5, and at static temperature and pressure values of 200 K and 70 kPa, for which G (first Rayleigh line) at inlet = 1 550 kg/m^{2}s, and T_t = 451.4 K. Two oblique shocks turn the flow through 10° and 8°, respectively; this leads to a flow at M = 1.77 upstream of the normal shock, after which deceleration is considered to take place isentropically, followed by heating along the second Rayleigh line after point 2; G for subsonic diffusion = 387.5 kg/m^{2}s. In Figure 7(a), the oblique shock compression line appears to follow the isentropic line fairly closely, as is confirmed by reference to Figure 7(b). The effect of η of the small entropy increase during compression is similar to that introduced by the imperfection η_c (to be discussed later).

Modified Joule cycle

In the simple Joule cycle, using isentropes,

$$\frac{T_2}{T_1} = \left(\frac{p_2}{p_1}\right)^{\frac{\gamma-1}{\gamma}} = \left(\frac{p_3}{p_4}\right)^{\frac{\gamma-1}{\gamma}} = \frac{T_3}{T_4}. \qquad (19)$$

Let $\tau = T_2 / T_1 = T_3 / T_4$ *so* $T_4 / T_1 = T_3 / T_2$.
In terms of static enthalpies, η is given by

$$\begin{aligned} \eta &= \frac{W}{Q} = \frac{C_p(T_3-T_4)-C_p(T_2-T_1)}{C_p(T_3-T_2)} \\ &= 1-\frac{T_4-T_1}{T_3-T_2} = 1-\frac{(T_4/T_1-1)T_1}{(T_3/T_2-1)T_2} \\ &= 1-1/\tau\,. \end{aligned} \qquad (20)$$

With inefficiencies (see [5]), if
$a = \eta_t\eta_c\theta$, $\theta = T_3 / T_1$, and $b = \eta_c(\theta - 1)$,
then

$$\eta_c = \frac{h_2-h_1}{h_2'-h_1} \text{ and } \eta_t = \frac{h_3-h_4'}{h_3-h_4}$$
$$\text{giving } \eta = \frac{(\tau-1)(a/\tau-1)}{b-\tau}. \qquad (21)$$

In the modified cycle, using a Rayleigh combustion line, let the combustion pressure change be expressed in terms of $\alpha :\Rightarrow p_3 = \alpha p_2$ and a useful relationship between α and mass velocity, G, is (see Appendix for derivation)

$$\alpha = \frac{(p_2+RT_1\tau G^2/p_2)\pm\left[(p_2+R\tau T_1G^2/p_2)^2-4(G^2R\theta T_1)\right]^{\frac{1}{2}}}{2p_2}, \qquad (22)$$

if G is known. Alternatively, G may be found from α, using

$$G = p_2\left[\frac{1-\alpha}{RT_1(\theta/\alpha-\tau)}\right]^{\frac{1}{2}} \qquad (23)$$

η may be found from (see Appendix)

$$\eta = \frac{\left\{\theta-\left[\tau^{\frac{1}{(1-\gamma)}}+p_1\tau^{\frac{\gamma}{(\gamma-1)}}(1-\alpha)/v_1G^2\right]\left[\alpha\tau^{\frac{\gamma}{(\gamma-1)}}\right]^{\frac{1}{\gamma}}\right\}-(\tau-1)}{\theta-\tau} \qquad (24)$$

Worked examples

For a simple cycle, letting $\tau = 2, \eta = 1-1/\tau = 0.5$, while, if $\eta_t = \eta_c = 0.9$, so that $b = 0.9(5-1) = 3.6$ if $\theta = 5$, and $a = 0.9 \times 0.9 \times 5 = 4.05$, this equation for η gives

$$\eta = \frac{(2-1)(4.05/2-1)}{3.6-2} = 0.641\,.$$

The example shown in Figure 8 makes use of the following parameters for the modified cycle:

T_a	=	288 K	$\alpha = 4$
p_a	=	1 bar	G = 181.56 kg/m^{2}s
M_2	=	0.135 (starting combustion chamber value)	
M_3	=	0.226 (final combustion chamber value)	
T_3	=	1 100 K	

Thermal choking does not occur until T^* = 4 317 K.

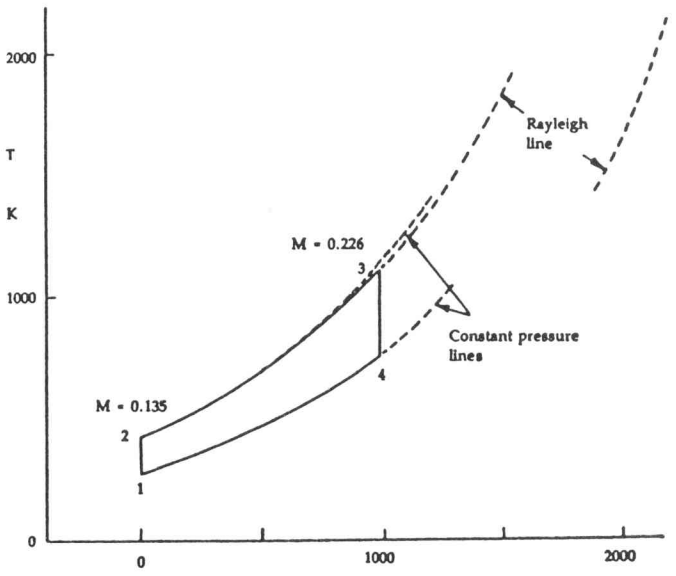

Figure 8(a) T-s diagram illustrating the modified Joule cycle.

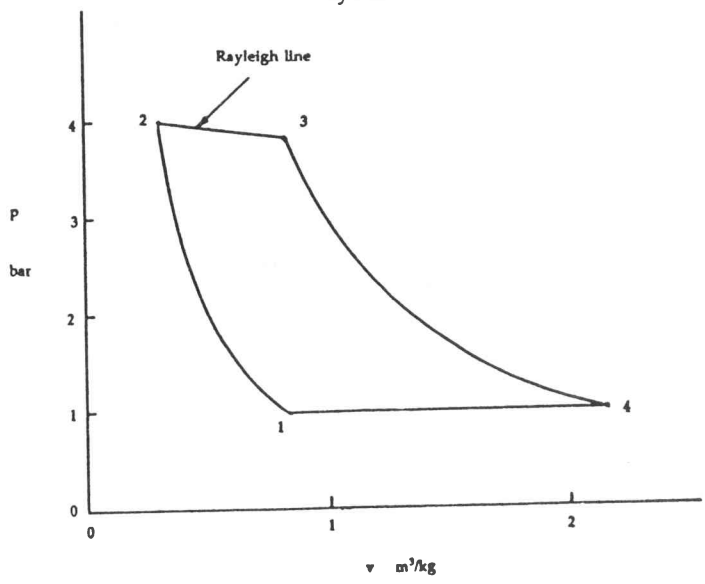

Figure 8(b) p-v diagram illustrating the modified Joule cycle.

Figure 9 illustrates the slow reduction in the theoretical value of η with increasing pressure drop for the modified cycle, using

$T_1 = 288$ K

$p_1 = 10^5$ Pa

$\theta = 5$

$\tau = 2$

Then, $\eta = 0.493$ at $\alpha = 0.971$, falling to $\eta = 0.469$ at $\alpha = 0.88$.

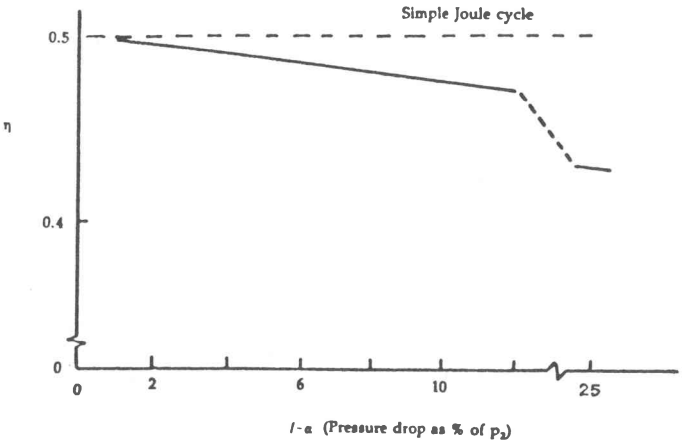

Figure 9 Cycle efficiency vs pressure drop in the modified Joule cycle.

The exit point 4 of the cycle normally represents a supersonic flow (e.g. $M_4 = 2.33$ for the cycle parameter values given). To reach such a value, the flow must pass through the sonic value which corresponds to the maximum s point on the appropriate Rayleigh curve. Such acceleration after the flow has left the combustion chamber corresponds to a decreasing and then increasing area (increasing and then decreasing G), i.e. the flow follows a series of G curves, on one of which it passes through a maximum entropy point as it goes sonic.

Discussion and Conclusions

1. Rayleigh lines, representing constant mass flow per unit area under conditions of heat transfer, are considered to be appropriate components of processes following the Joule cycle (in which two elements are constant pressure lines). This technique may also be applied to other cycles embodying constant pressure lines. Variation of combustion chamber cross-sectional area or mass flow produces little change in the subsonic branches of Rayleigh lines on a T-s plot (and there is even closer correspondence on a T_t-s plot). This small change in the cycle on T-s ordinates implies little effect on heat reception or rejection.

2. Both Rayleigh lines and the use of the conventional mass flow parameter, $\dot{m}\,(RT_t)^{\frac{1}{2}} / p_t$, lead to a linear pressure drop on a p-v plot. The subsonic Rayleigh line may hence be arranged by adjustment of mass velocity, G, to coincide with any experimental pressure drop (such as a '4% line') obtained in normal practice. η may then be calculated as indicated for the modified cycle. As an example, if the pressure at the end of combustion is only, say, 3% less than the pressure at entrance to the combustion chamber, η does not decrease more than 1% from the simple Joule cycle value of 50%. If p_3 is10% less than p_2, η drops to 47.5%, which indicates the importance of holding down combustion chamber losses by a suitable choice of mass velocity.

References

[1] JL Kerrebrock. *Aircraft Engines and Gas Turbines.* M.I.T., 1977.

[2] MJ Zucrow. *Aircraft and Missile Propulsion*, Vol. I. Wiley, 1958.

[3] MJ Zucrow. *Aircraft and Missile Propulsion*, Vol. II. Wiley, 1958.

[4] H Cohen, GFC Rogers & HIH Saravanamuttoo. *Gas Turbine Theory*, 3rd edn. Longman, 1987.

[5] GHA Cole. *Thermal Power Cycles.* Edward Arnold, 1991.

[6] GC Oates. *Aircraft Propulsion Systems, Technology and Design.* AIAA, 1989.

[7] P Hill & C Peterson. *Mechanics and Thermodynamics of Propulsion,* 2nd edn. Addison-Wesley, 1992.

[8] AB Çambel & BH Jennings. *Gas Dynamics.* McGraw-Hill, 1958.

[9] AB Çambel. Section 8 Compressible Flow. In VL Streeter, *Handbook of Fluid Dynamics*, 1st edn. McGraw-Hill, 1961.

Appendix

Derivation of Parameters η and α

Using isentropic compression and expansion, let $T_2 = \tau T_1$. Then

$$\left(\frac{p_2}{p_1}\right)^{\frac{\gamma-1}{\gamma}} = \frac{T_2}{T_1} = \tau \text{ so } \frac{p_2}{p_1} = \tau^{\frac{\gamma}{\gamma-1}} \text{ or } p_2 = p_1\tau^{\frac{\gamma}{\gamma-1}}$$
$$\text{and } \frac{p_1}{p_2} = \left(\frac{v_2}{v_1}\right)^{\gamma} \text{ so } v_2 = v_1\tau^{\frac{1}{\gamma-1}} \quad (1)$$

Let p_3 drop to αp_2 during combustion.[1] For a Rayleigh line,

$$v_3 - v_2 = \frac{p_3 - p_2}{-G^2} \quad (2)$$

$$\Rightarrow v_3 = v_2 + \frac{p_2(\alpha - 1)}{-G^2} = v_2 + \frac{p_2(1-\alpha)}{G^2} \quad (3)$$

Let the gas be heated to $T_3 = \theta T_1$. Then $T_3 - T_2 = T_1(\theta - \tau)$. Also,

$$\frac{p_3}{p_4} = \left(\frac{v_4}{v_3}\right)^{\gamma}. \text{ Since } p_4 = p_a = p_1, \quad (4)$$

$$\frac{v_4}{v_3} = \left(\frac{p_3}{p_1}\right)^{\frac{1}{\gamma}}, \text{ whence} \quad (5)$$

$$v_4 = v_3(p_3/p_1)^{\frac{1}{\gamma}} = \left[v_2 + \frac{p_2(1-\alpha)}{G^2}\right]\left[\frac{\alpha p_2}{p_1}\right]^{\frac{1}{\gamma}}. \quad (6)$$

Now,

$$v_2 = v_1\tau^{\frac{1}{1-\gamma}} \text{ and } p_2/p_1 = \tau^{\frac{\gamma}{\gamma-1}}, \quad (7)$$

$$\Rightarrow v_4 = \left[v_1\tau^{\frac{1}{1-\gamma}} + \frac{p_1\tau^{\frac{1}{\gamma-1}}(1-\alpha)}{G^2}\right]\left[\alpha\tau^{\frac{\gamma}{\gamma-1}}\right]^{\frac{1}{\gamma}} \quad (8)$$

$$\Rightarrow T_4 = \frac{p_1 v_4}{R}$$
$$= \frac{p_1}{R}\left[v_1\tau^{\frac{1}{1-\gamma}} + \frac{p_1\tau^{\frac{\gamma}{\gamma-1}}(1-\alpha)}{G^2}\right]\left[\alpha\tau^{\frac{\gamma}{\gamma-1}}\right]^{\frac{1}{\gamma}} \quad (9)$$

$$\Rightarrow T_3 - T_4$$
$$= \theta T_1 - \frac{T_1}{v_1}\left[v_1\tau^{\frac{1}{1-\gamma}} + \frac{p_1\tau^{\frac{\gamma}{\gamma-1}}(1-\alpha)}{G^2}\right]\left[\alpha\tau^{\frac{\gamma}{\gamma-1}}\right]^{\frac{1}{\gamma}} \quad (10)$$
$$= \theta T_1 - T_1\left[\tau^{\frac{1}{1-\gamma}} + \frac{p_1}{v_1}\frac{\tau^{\frac{\gamma}{\gamma-1}}(1-\alpha)}{G^2}\right]\left[\alpha\tau^{\frac{\gamma}{\gamma-1}}\right]^{\frac{1}{\gamma}}$$

$$\Rightarrow \eta = \frac{W_{34} - W_{12}}{Q_{32}} = \frac{C_p(T_3 - T_4) - C_p(T_2 - T_1)}{C_p(T_3 - T_2)}$$

$$= \frac{\left\{T_1\theta - T_1\left[\tau^{\frac{1}{1-\gamma}} + \frac{p_1}{v_1}\tau^{\frac{\gamma}{\gamma-1}}(1-\alpha)/G^2\right]\left[\alpha\tau^{\frac{\gamma}{\gamma-1}}\right]^{\frac{1}{\gamma}}\right\} - T_1(\tau-1)}{T_1(\theta-\tau)}$$

$$= \frac{\left\{\theta - \left[\tau^{\frac{1}{1-\gamma}} + \frac{p_1}{v_1}\tau^{\frac{\gamma}{\gamma-1}}(1-\alpha)/G^2\right]\left[\alpha\tau^{\frac{\gamma}{\gamma-1}}\right]^{\frac{1}{\gamma}}\right\} - (\tau-1)}{(\theta-\tau)} \quad (11)$$

If G is known, α may be found as follows as

$f(p_2, R, \tau, T_1, G, \theta)$:

$p_3 v_3 = RT_3 = R\theta T_1$ and $p_2 v_2 = RT_2 = R\tau T_1$

$\Rightarrow v_3 = R\theta T_1/p_3$ and $v_2 = R\tau T_1/p_2$.

Now, $p_3 - p_2 = (v_3 - v_2) - G^2$

$\Rightarrow p_3 = p_2 - (v_3 - v_2)G^2$

$= p_2 - G^2 R\theta T_1/p_3 + R\tau T_1 G^2/p_2$.

$$\Rightarrow p_3 + \frac{G^2 R\theta T_1}{p_3} = p_2 + \frac{R\tau T_1 G^2}{p_2}. \quad (12)$$

Putting $p_3 = \alpha p_2$,

$$\alpha p_2 + \frac{G^2 R\theta T_1}{\alpha p_2} = p_2 + \frac{R\tau T_1 G^2}{p_2} \text{ whence,} \quad (13)$$

$$\alpha^2 p_2 + G^2 R\theta T_1/p_2 = \alpha\left(p_2 + R\tau T_1 G^2/p_2\right) \text{ or} \quad (14)$$

$$\alpha^2 p_2 - \alpha\left(p_2 + R\tau T_1 G^2/p_2\right) + G^2 R\theta T_1/p_2 = 0 \text{ whence,} \quad (15)$$

$$\alpha = \frac{\left(p_2 + RT_1\tau G^2/p_2\right) \pm \left[\left(p_2 + R\tau T_1 G^2/p_2\right)^2 - 4\left(G^2 R\theta T_1\right)\right]^{\frac{1}{2}}}{2p_2}, \quad (16)$$

(the positive root being the applicable one). Alternatively, given α_2 :

$v_2 = RT_2/p_2 = R\tau T_1/p_2$; $v_3 = RT_3/p_3 = R\theta T_1/\alpha p_2$.

$$\Rightarrow v_3 - v_2 = \frac{R\theta T_1}{\alpha p_2} - \frac{R\tau T_1}{p_2} = \frac{RT_1}{p_2}\left(\frac{\theta}{\alpha} - \tau\right)$$
$$\Rightarrow G = \left[\frac{p_2 - p_3}{v_3 - v_2}\right]^{\frac{1}{2}} = \left[\frac{(1-\alpha)p_2^2}{RT_1\left(\frac{\theta}{\alpha} - \tau\right)}\right]^{\frac{1}{2}} = p_2\left[\frac{1-\alpha}{RT_1\left(\frac{\theta}{\alpha} - \tau\right)}\right]^{\frac{1}{2}} \quad (17)$$

$$= p_1\tau^{\frac{\gamma}{\gamma-1}}\left[\frac{1-\alpha}{RT_1\left(\frac{\theta}{\alpha} - \tau\right)}\right]^{\frac{1}{2}}. \quad (18)$$

[1] A derivation of $\alpha = f(p_2, R, \tau, T_1, G, \theta)$ is given below.